IEEE Access
Multidisciplinary | Rapid Review | Open Access Journal

Received 1 April 2024, accepted 16 April 2024, date of publication 22 April 2024, date of current version 30 April 2024.

Digital Object Identifier 10.1109/ACCESS.2024.3391890

RESEARCH ARTICLE

Realization of Robust Frequency Stability in Low-Inertia Islanded Microgrids With Optimized Virtual Inertia Control

WALEED M. HAMANAH[1,2], MD. SHAFIULLAH[3,4], (Senior Member, IEEE), LUAI M. ALHEMS[1], MD. SHAFIUL ALAM[5], AND MOHAMMAD A. ABIDO[2,3,6], (Senior Member, IEEE)

[1]Applied Research Center for Metrology, Standards and Testing, Research and Innovation, KFUPM, Dhahran 31261, Saudi Arabia
[2]Department of Electrical Engineering, College of Engineering and Physics, KFUPM, Dhahran 31261, Saudi Arabia
[3]Control and Instrumentation Engineering, College of Engineering and Physics, KFUPM, Dhahran 31261, Saudi Arabia
[4]Interdisciplinary Research Center for Sustainable Energy Systems (IRC-SES), KFUPM, Dhahran 31261, Saudi Arabia
[5]Applied Research Center for Environment and Marine Studies, Research and Innovation, KFUPM, Dhahran 31261, Saudi Arabia
[6]SDAIA-KFUPM Joint Research Center for Artificial Intelligence, KFUPM, Dhahran 31261, Saudi Arabia

Corresponding author: Waleed M. Hamanah (waleed.hamanah@kfupm.edu.sa)

The author would like to acknowledge the support provided by the Applied Research Center for Metrology, Standards and Testing (ARC-MST) and the Deanship of Research Oversight and Coordination (DROC), through Grant No. INRE2330, Research and Innovation, King Fahd University of Petroleum and Minerals (KFUPM).

ABSTRACT The increase in renewable energy resources penetration into microgrids weakens the inertia of microgrids and negatively affects their frequency stability. This reduction in inertia reduces the microgrid's ability to handle disturbances and increases frequency instability risk. The purpose of this paper is to present a virtual inertia (VI) control strategy for an island microgrid with the use of an energy storage system (ESS) to improve inertia and frequency stability of the system. The VI controller parameters are optimized using the differential evolution (DE) algorithm. The proposed VI control strategy can effectively improve microgrid frequency stability and reduce the risk of frequency instability. The results demonstrate that the proposed strategy is effective and can provide fast and reliable virtual inertia support for the microgrid. The proposed VI control approach is verified through simulation results and performs better than the conventional inertial response for frequency stability in islanded microgrids. Virtual inertia control injects/absorbs active power into/from the microgrid during frequency deviations. Different disturbances are applied to demonstrate uncertain load and RES generation behavior. The proposed VI control method is compared with the available literature. In the proposed method, the frequency deviation is better controlled. Furthermore, the results demonstrate a more stable and efficient system operation with the developed VI controller than the existing methods.

INDEX TERMS Virtual inertia control, differential evolution algorithm, energy storage systems, microgrid, renewable energy resources.

ABBREVIATIONS

AC	Alternating current.
ACE	Area Control Error System.
AI	Artificial Intelligence.
CR	Crossover Factor.
DC	Direct current.
DE	Differential Evolution Algorithm.
ESS	Energy Storage System.
GRC	Governor Generator Rate Constraint.
ISE	Integral of the Squared Error.
MGs	Microgrids.
PLL	Phase-locked loop.
PSO	Particle swarm optimization.
PV	Photovoltage.

The associate editor coordinating the review of this manuscript and approving it for publication was Lei Chen.

RoCoF	Rate of Change of Frequency.
VI	Virtual Inertia.
VSG	Virtual Synchronous Generator.

I. INTRODUCTION

The adoption of microgrids (MGs) that integrate more renewable energy sources (RESs) has recently increased. As such, MGs constitute a significant part of the current transition away from traditional energy sources. The low-inertia nature of these MGs has implications for dynamic stability, such as a transient power impact and unacceptable frequency variation due to RESs' highly variable characteristics [1], [2]. To mitigate these dynamic stability issues, advanced control and optimization algorithms, such as model predictive control [3] and artificial intelligence (AI) [4], are being proposed for MG operation. RES penetration correlates with decreasing virtual inertia [5]. Increased penetration of renewable energy leads to the wide application of power electronics converters. Power converters reduce the syste's inertia, resulting in stability issues and frequency fluctuations [4]. The use of AI algorithms can also enhance dynamic stability and restore virtual inertia, improving the reliability of power systems [6]. DGs replace conventional synchronous generators in microgrids with distributed power generation, affecting frequency stability negatively [7]. To address these stability issues, advanced control strategies and methods should be used to improve the frequency and voltage stability of the microgrids. Two-layer multiple model predictive control method was used in [8]. A microgrid with renewable energy and ESS was evaluated for frequency performance. However, there are some drawbacks to this method as well. First, it requires significant computational resources to implement. Second, it can be difficult to tune the parameters of the algorithm to get good performance. A virtual adaptive inertia control based on fuzzy logic was presented in [9]. Using the dual extended Kalman filter, the authors estimated the states of energy storage battery packs online. However, online estimation could be computationally intensive, which could lead to delays in the control system.

To address the issue of low inertia, several techniques have been proposed. VI is one of the main techniques for providing additional inertia in power systems [10]. The VI offers an effective solution to increase the inertia in power systems, allowing them better control over their operations. Simulating virtual inertia can give more inertia to the MG, allowing for higher penetration of RESs. An advanced control inverter and Energy Storage System (ESS) can enhance the system's inertia, which in turn improves the system's stability [11]. Furthermore, using virtual inertia can improve the power quality of the system and make it more reliable and resilient in times of disturbance. Virtual inertia control and its application have been proven to provide uninterruptible power to microgrids which enhances the system's stability [6], [12], [13]. Additionally, using virtual inertia to improve power quality and increase reliability is becoming increasingly popular in the industry. According to [14] and [15], a novel LFC design for hydro-hydro systems based on fuzzy logic was presented, with a particle swarm optimization (PSO) PID that was viably optimized into a new and robust Fuzzy-PSO-PID.

Several VI control methods have been implemented in the literature to enhance inertia control for MG frequency response. Furthermore, these methods can be developed to provide optimal frequency response for large and small disturbances. VI synthesizes the inertia property in a microgrid [16]. Moreover, virtual inertia can be used to improve the frequency response of microgrids in conjunction with conventional inertia control approaches. This is accomplished through a supplementary simulated control loop. This improves the frequency response of the microgrid under high-RES penetration and low inertia by adding power to a standard load. Adding virtual inertia to the microgrid improves its frequency response, thus providing a reliable energy source under varying conditions. For instance, derivative VI control has been studied for a hybrid microgrid with both wind and PV sources by the authors of [17] and [18]. These papers did not optimize the values of the VI controller parameters. The authors of [19] proposed a technique for VI emulation and damping, which enhances system inertia, thereby meeting the desired frequency response. To address this issue, [19] proposed a method for optimizing the VI controller parameters, thus allowing for improved frequency response and stability of the hybrid microgrid. The authors of [20] utilized voltage-dependent loads coupled with electric spring technology as smart loads for enhancing the system's inertia. There is evidence that virtual inertia can be controlled and improved by utilizing the virtual synchronous generator (VSG), which improves the voltage and frequency of weak (low-inertia) MGs [21], [22], [23], [24], [25], [26]. Similarly, using VSG technology can also help improve the syste's stability, allowing for greater control and responsiveness in the network. Using genetic algorithms, [27] optimized the derivative VI control system to improve MG inertia. The system can benefit from increased stability and enhanced virtual inertia control by implementing such strategies. The authors used an energy storage system to serve as virtual inertia for the microgrid. A coordination strategy for PV's virtual inertia and frequency damping control has been developed to achieve optimal frequency response [28]. Moreover, the process was found to have improved frequency regulation and enhanced the system's ability to withstand disturbances. The authors in [29] utilized ultra-capacitors for synthesizing virtual inertia. The authors of the research papers [30], [31], [32], [33], [34] proposed virtual inertia control for wind power only. The proposed methods have been tested and evaluated experimentally by the authors in [35] and [36], with their results confirming the successful implementation of the strategy. The papers did not consider more complex systems with high penetration of RES. The

authors of [35] proposed a synchronous power controller for synthesizing virtual inertia from a PV system. The authors further explored the potential of virtual inertia control for more complex systems with high penetration of RES, and their results confirmed the successful implementation of the strategy. This technique was used by [36] for large-scale PV plants. Furthermore, the authors showed that the method could be effectively applied to larger systems, with applications to large-scale PV plants. However, these solutions did not optimize the parameters of the controllers. This paper solves the weak inertia problem of an island microgrid with RES penetration by a VI control loop that improves the frequency. Different signals (constant, unit, and random step) were used to demonstrate a variety of load/RES scenarios (wind and PV resources). To this end, a VI approach was proposed to optimize the frequency regulation of the system, which was demonstrated with different load/RES scenarios and input signals. A differential evolution algorithm is used to optimize the controller parameters. Using the proposed VI approach and the DE algorithm, the frequency regulation of the system was successfully optimized for a wide range of load/RES scenarios and various input signals. The system's frequency response was examined to show how the proposed VI control system suppresses the frequency deviation caused by low inertia. A comparison was carried out with a conventional VI controller. Moreover, the proposed controller yielded more efficient frequency regulation than the traditional VI controller, with a reduced settling time and steady-state error. Another comparison was carried out with other VI control techniques proposed in the past literature. The MATLAB/SIMULINK platform was used for simulations and system verification purposes. As a result, the proposed controller showed superior performance to the conventional VI controller and other VI control techniques presented in the past literature, as evidenced by its reduced settling time, steady-state error, and greater efficiency in frequency regulation.

Throughout the paper, the following structure is followed. This structure provides the foundation for the arguments and evidence presented in the article. The microgrid system configuration in Section II, along with an overview of the existing work, while the microgrid system model and proposed derivative structure is presented in Section III. VI control system is presented in Section IV. The differential evolution algorithm and the methodology is outlines in Section V. Finally, the simulation and results are discussed in detail in Section VI, along with a conclusion in Section VII.

II. MICROGRID SYSTEM CONFIGURATION

Accurate microgrid system modeling and configuration enables improved system performance and reliability. A thorough understanding of microgrid systems requires appropriate modeling and configuration techniques to ensure efficient operations. To further ensure efficient operations, it is essential to have an in-depth knowledge of microgrid system modeling and configuration practices.

A. MICROGRID MODELLING

The microgrid's practical dynamics were accurately modeled using a microgrid with different types of generation and load in the study. These include 15MW generating units (thermal), 9MW wind farm (wind turbine), 8MW solar PV, 5MW ESS, 6MW residential loads, and 12MW industrial load. This setup is shown in Figure 1. In the model, the solid line represents the power line used for electrical power trading. In contrast, the dashed line represents the communication line that is used to control and status information exchange with the primary grid. A phase-locked loop (PPL) control system generates an output signal whose phase is related to an input signal's phase. The PPL system compares the phase of the input signal to the phase of the output signal and adjusts the output signal phase accordingly. It is used to synchronize signals in communication systems and other electronic circuits.

B. DESCRIPTION OF THE VI CONTROL

Virtual inertia (VI) control is a technique used in augmented reality to enhance immersion and realism. It involves creating the illusion of inertia in a virtual environment, giving users the same physical sensations they would experience in a real setting. This is achieved by manipulating virtual objects' properties to simulate their real-world behavior. To make a power imbalance, a disturbance is applied to the microgrid, which results in frequency deviation. For the primary frequency control, the governor's action minimizes the frequency deviation of the microgrid from 10 seconds to 30 seconds. Afterward, the secondary frequency controls the dynamic response and takes the frequency to the nominal value from 30 seconds to 30 mins [3]. Before the primary inertia control action, the inertia response uses the energy stored in the rotors of the generating sources to balance the power requirement in the first 10 secs. However, the inertial response is poor in the first 10 secs due to the low inertia of the renewable energy sources. This leads to a faster rate of change of frequency (RoCoF) and higher frequency deviation [4]. Consequently, there is the chance that frequency relays would trip, load curtailment, or cascade outages in the microgrid due to low inertia [3]. Thus, synthesized inertia or VI must be injected into the system to counter the low inertia problem. The inertia of the system is a measure of the overall kinetic energy stored in the rotating mass (E_K) and is given by [17]:

$$E_K = \frac{1}{2} J\omega^2 \tag{1}$$

where, J is system inertia (Kg/m^2), and ω is the angular frequency (rad/s). Considering the swing equation, one has:

$$J\omega \frac{d\omega}{dt} = P_m - P_l \tag{2}$$

where, P_m and P_L are the mechanical and load power, respectively. The inertia constant of the system, H is expressed as:

$$H = \frac{E_k}{S} = \frac{J\omega^2}{2S} \tag{3}$$

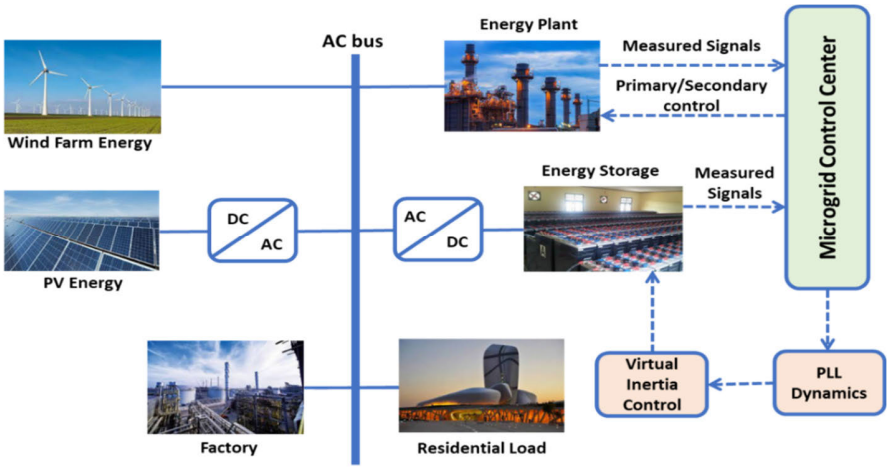

FIGURE 1. Islanded microgrid model.

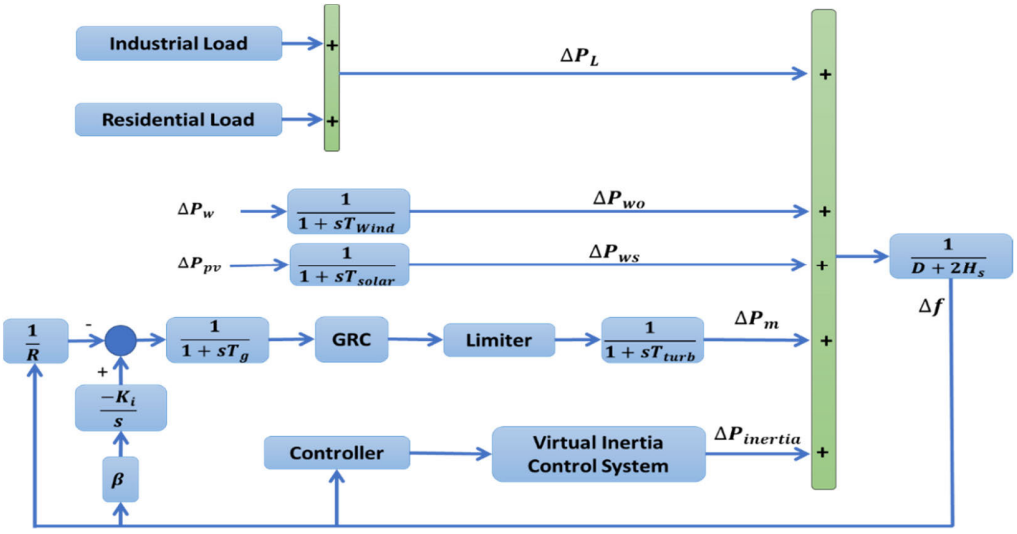

FIGURE 2. VI control strategy of an island microgrid with high renewable energy penetration.

where, S stands for the apparent power (VA). Therefore, equation (2) can be rewritten as:

$$\frac{2H}{f}\frac{df}{dt} = \frac{P_m - P_l}{S} \tag{4}$$

where df/dt is the RoCoF of the system.

III. MICROGRID SYSTEM MODELIN

Microgrid system modeling proposals integrate a virtual impedance loop and voltage droop control to produce a derivative VI control structure. This control structure aims to enhance the stability and performance of the microgrid system by effectively managing power flow and maintaining voltage and frequency within the desired limits.

A. THE PROPOSED DERIVATIVE VI CONTROL STRUCTURE

The dynamic structure of the MG considering the dynamic effects of VI control with frequency measurement is shown in ***Figure 2.*** Frequency analysis is conducted on the system. The low-dynamic model is developed based on [20] and [21]. Governor generator rate constraint (GRC) and turbine valve gate closing/opening rate (Vu, VL) are used, which adds non-linearity to the system. The domestic load is balanced by the generating unit (thermal), and the thermal power plant provides the primary frequency control. The steady-state frequency error for secondary frequency control is removed by the area control error (ACE) system. The ESS emulates the virtual inertia loop. Renewable power is supplied to the grid by wind and solar PV, and they do not provide frequency control. The sources of external disturbances to the system are RES and domestic loads (domestic and industrial).

Figure 3 shows the derivative VI controller. The control system calculates the RoCoF. Virtual damping was not considered in the design of the VI control loop for RoCoF control, as seen in [19], [20], and [21]. In this study, both inertia K_{VI} and damping D_{VI} have been considered in the

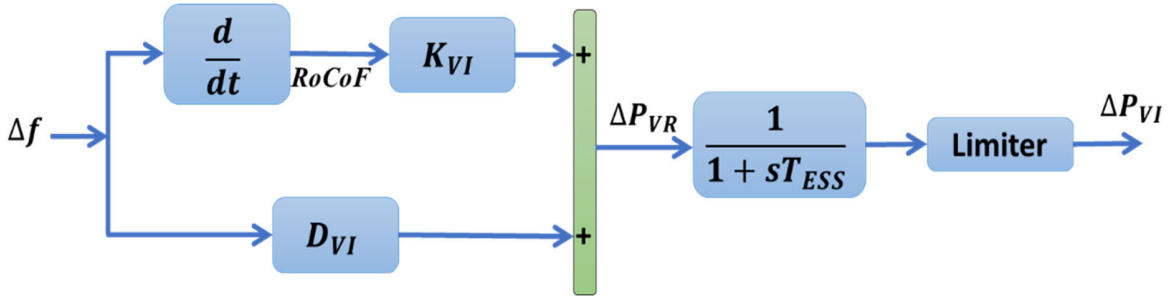

FIGURE 3. Dynamic structure RoCoF controller.

design in order to control both RoCoF $(d(\Delta f)/dt)$ and Δf. Cheap and simple design is used in this study by using PI controller as the designed controller. The ESS provides VI power ΔP_{VI} during power imbalance. For frequency regulation to be maintained, the amount of power exchanged with the ESS to cancel power imbalance is determined by the VI loop (derivative D_{VI} and K_{VI}). The VI power proportional to Δf and RoCoF are generated by D_{VI} and K_{VI} respectively. During a frequency deviation, the virtual inertia control system adds the required power to the microgrid.

$$\Delta P_i = \frac{\Delta P_{VI}}{1 + sT_{VI}} \frac{d(\Delta f)}{dt} \tag{5}$$

where T_{VI} is the VI time constant of the added filter, K_{VI} is the control gain of the VI controller, and Δf is the system frequency deviation.

B. STATE SPACE MODEL

The microgrid system is described by the following set of linear equations for analysis purposes [6]:

$$\Delta P_m = \frac{1}{1+sT} \times \Delta P_g \tag{6}$$

$$\Delta P_{pv} = \frac{1}{1+sT_{solar}} \times \Delta P_{solar} \tag{7}$$

$$\Delta P_w = \frac{1}{1+sT_{WT}} \times \Delta P_{wind} \tag{8}$$

$$\Delta P_g = \frac{1}{1+sT_g} \times \left[\Delta P_{ACE} - \frac{1}{R}\Delta f\right] \tag{9}$$

$$\Delta P_{ACE} = \frac{ACE}{s} = -\frac{k_i}{s}[\beta.\Delta f] \tag{10}$$

$$\Delta f = \frac{1}{2Hs + D}\begin{pmatrix}\Delta P_m + \Delta P_{pv} + \Delta P_w \\ +\Delta P_{inertia} - \Delta P_L\end{pmatrix} \tag{11}$$

$$\Delta P_i = \frac{1}{1+sT_{WT}} \times \left[D_{VI}\Delta f + \frac{d(\Delta f)}{dt}\right]$$

$$\Delta P_i = \frac{\Delta P_{VR}}{1+sT_{WT}} \tag{12}$$

where, $\Delta P_{pv} = D_{VI}\Delta f + \frac{d(\Delta f)}{dt}$, where ΔP_m, is the output power from the the thermal power station, ΔP_{pv} is denote the solar photovoltaic, ΔP_w is wind farm, and ΔP_g is turbine governor, the variation in solar power is ΔP_{Solar}, the variation in wind power is ΔP_W, and the variation in load demand is ΔP_L. ΔP_f is the system frequency deviation. ΔP_i is the power injected into grid due to inertia emulation, also, the the virtual damping is D and H is the the inertia. So, the state vector is defined as:

$$x = \left[\Delta P_m\ \Delta P_{pv}\ \Delta P_w\ \Delta P_g\ \Delta P_C\ \Delta P_f\ \Delta P_i\right]^T$$

and the disturbance input vector is given by:

$$x = [\Delta P_{Solar}\ \Delta P_W\ \Delta P_L]^T$$

The control input is set as follows: $U = \Delta P_{V\ R}$ and the output is set as: $y = \Delta f$

Then, the state space representation of the microgrid system can be written as:

$$\dot{x} = Ax + \Gamma\delta + BU$$

$$A = \begin{bmatrix} -\frac{1}{T_t} & 0 & 0 & \frac{1}{T_t} & 0 & 0 & 0 \\ 0 & -\frac{1}{T_{WT}} & 0 & 0 & 0 & 0 & 0 \\ 0 & 0 & -\frac{1}{T_{pv}} & 0 & 0 & 0 & 0 \\ 0 & 0 & 0 & -\frac{1}{T_g} & \frac{1}{T_g} & -\frac{1}{RT_g} & 0 \\ 0 & 0 & 0 & 0 & -K_i\beta & 0 & 0 \\ \frac{1}{2H} & \frac{1}{2H} & \frac{1}{2H} & 0 & 0 & \frac{D}{2H} & \frac{1}{2H} \\ 0 & 0 & 0 & 0 & 0 & 0 & -\frac{1}{T_{WT}} \end{bmatrix}$$

$$B = \begin{bmatrix} 0 & 0 & 0 \\ 0 & \frac{1}{T_{WT}} & 0 \\ \frac{1}{T_{pv}} & 0 & 0 \\ 0 & 0 & 0 \\ 0 & 0 & 0 \\ 0 & 0 & -\frac{1}{2H} \\ 0 & 0 & 1 \end{bmatrix}, \Gamma = \begin{bmatrix} 0 \\ 0 \\ 0 \\ 0 \\ 0 \\ 0 \\ \frac{1}{T_{VI}} \end{bmatrix} \tag{13}$$

C. ANALYSIS OF THE MICROGRID SYSTEM UNDER THE VI CONTROLLER

The simplified version of the proposed VI controller is shown in Figure 4, which is derived from ***Figure 2*** and Figure 3. Using Figure 3, the following can be formulated

$$\Delta f = \frac{1}{2Hs + D}\left(\Delta P_g - \Delta P_L \pm \Delta P_{VI}\right) \tag{14}$$

where, $\Delta P_g$is the total generated power.

$$\Delta P_{VI} = \Delta P_{VR}\frac{1}{1+sT_{ESS}} \tag{15}$$

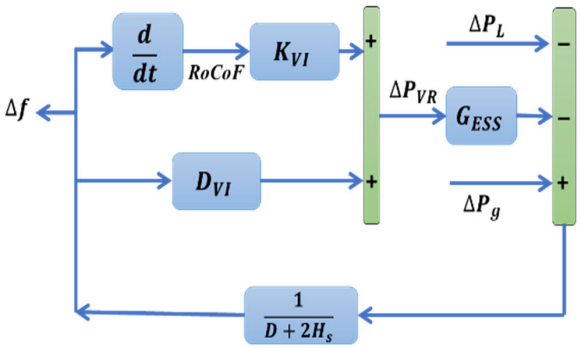

FIGURE 4. The simplified dynamic model controller.

$$\Delta f = \frac{1}{2Hs + D}\left(\Delta P_g - \Delta P_L \pm \Delta P_{VR}\frac{1}{1 + sT_{ESS}}\right) \tag{16}$$

$$\Delta f = \frac{1}{\Pi}\left(\Delta P_g - \Delta P_L \pm \Delta P_{VR}\frac{1}{1 + sT_{ESS}}\right) \tag{17}$$

where, $\Pi = 2Hs + D$, and for a step load change,

$$\Delta P_L(s) = \frac{\Delta P_L}{s}$$

The function will be:

$$\Delta f_{SS} = \lim_{s\to 0} s\Delta f = \frac{\Delta P_{gSS} - \Delta P_L \pm \Delta P_{VISS}}{\Pi(0)} \tag{18}$$

where, $\Delta P_{gSS} = \lim_{s\to 0} s\Delta P_g$, $\Pi\,(0) = D$

$$\Delta P_{gSS} = \lim_{s\to 0} s\Delta P_{VR} = \left(\frac{1}{1 + sT_{ESS}}\right) \tag{19}$$

The frequency deviation under a steady state becomes

$$\Delta f_{SS} = \lim_{s\to 0} s\Delta f = \frac{\Delta P_{gSS} - \Delta P_L \pm \Delta P_{VISS}}{D} \tag{20}$$

To have zero frequency deviation, (21) must be fulfilled.

$$\Delta P_L = \Delta P_{gSS} \pm \Delta P_{VISS} \tag{21}$$

The VI controller makes the frequency deviation zero to balance the generated and VI powers with the changes in the load demand.

$$T_{MG_{withVI}} = \left(\frac{\delta f}{\Delta P_L}\right)_{mg_{VI}} = \frac{-\left(\frac{1}{D+2Hs}\right)}{\left[\begin{array}{l} 1 + \Delta P_g\left(\frac{1}{D+2Hs}\right) \\ \pm\,(D_{VI} + sK_{VI})\left(\frac{1}{1+sT_{ESS}}\right)\left(\frac{1}{D+2Hs}\right)\end{array}\right]} \tag{22}$$

The transfer function of the microgrid without a VI controller is:

$$T_{MG_{withoutVI}} = \left(\frac{\Delta f}{\Delta P_L}\right)_{mg_{VI}} = \frac{-\left(\frac{1}{D+2Hs}\right)}{1 + \Delta P_g\left(\frac{1}{D+2Hs}\right)} \tag{23}$$

Thus, the overall function becomes:

$$T_{MG\_with\_VI} = \frac{-\left(\frac{1}{D+2Hs}\right)}{\left[\begin{array}{l}\left(T_{MG_{withoutVI}}\right)^{-1} \\ \pm\,(D_{VI} + sK_{VI})\left(\frac{1}{1+sT_{ESS}}\right)\end{array}\right]} \tag{24}$$

Therefore, the sensitivity of the microgrid with a VI control loop concerning the microgrid without a VI control loop is:

$$S^{MG_{withVI}}_{MG_{withoutVI}} = \left(\frac{\delta T_{MG_{withVI}}}{\delta T_{MG_{withoutVI}}}\right) \Big/ \left(\frac{T_{MG_{withVI}}}{T_{MG_{withoutVI}}}\right) \tag{25}$$

IV. VIRTUAL INERTIA CONTRO

A virtual synchronous generator mimics the actions of a prime mover. This provides a way for electricity to be generated without physical machinery. By injecting the required additional active power into the microgrid, VI control enhances the frequency stability of the microgrid by computing the RoCoF during contingencies [37]. Reactive power is required to maintain voltage to deliver active power. So, reactive power is flowing from the utility grid (source) to the loads based on a sending end voltage greater than the receiving end voltage. Therefore, if the sending end voltage is greater than the receiving end voltage, reactive power will flow from the source to the loads. In this way, virtual synchronous generators can help ensure a reliable and efficient power supply from microgrids with improved frequency stability. Furthermore, to solve the problem of hypersensitivity to noise in derivative control during frequency measurements, a low-pass filter is added to VI control [38], [39]. With this additional filter, VI control can effectively reduce the sensitivity of the system to sudden disturbances, providing improved frequency stability and a reliable power supply. Furthermore, the low-pass filter simulates the fast response (dynamic behavior) of the ESS. In this way, the VI control increases the system's inertia even though there is high penetration of RES. This ensures that the system can maintain frequency stability and a steady power supply, even under sudden disturbances and increased penetration of RES. Thus, ESS imitates inertia. As shown in Figure 2, the control system has the following block diagram. On the other hand, Figure 3 illustrates the RoCoF controller.

V. DIFFERENTIAL EVOLUTION STRATEGY

An important part of the DE algorithm is to optimize the parameters of the VI controller in order to achieve the best results. The DE algorithm is able to quickly search through a large parameter space to find the optimal solution. It is also able to handle complex, non-linear problems. This makes the DE algorithm an ideal choice for optimizing the VI controller parameters. Figure 5 illustrates the flowchart of the DE algorithm. The initial population (Np) is randomly generated from the given range in the first stage between two bounds (X_{min}, X_{max}). Then, each member of the initial population is evaluated using the fitness function [40], [41]. A solution

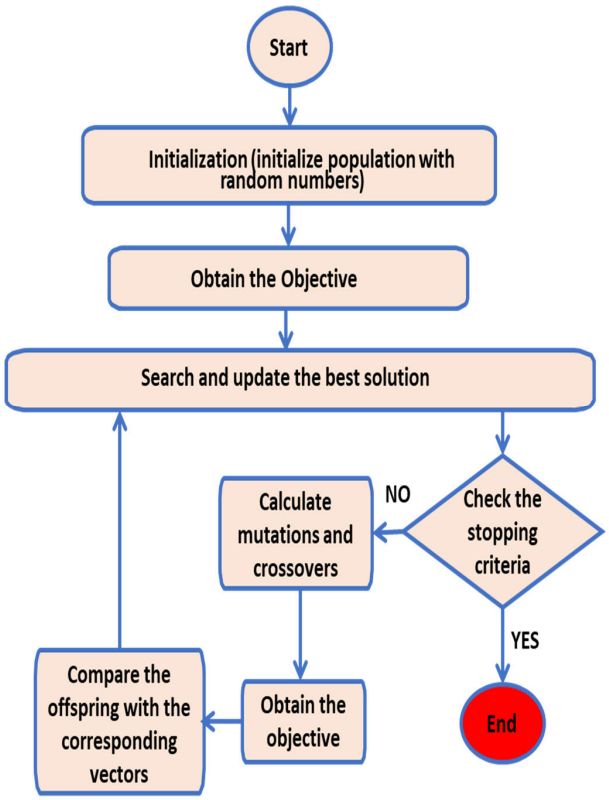

FIGURE 5. Differential evolution algorithm.

(X) consists of (D) elements, which are the dimensions of the problem (number of parameters to optimize). Finally, the best-fit individuals are selected for further optimization. In DE, factors that need to be defined include mutation factor (F) that controls the convergence speed and crossover factor (CR) that smoothens the convergence and ensures the solution diversity to avoid premature convergence and getting trapped into a local minimum during the process. The algorithm also specifies the maximum generation (Ng) during the initialization [42]. Therefore, the combination of mutation factor, crossover factor, and generation number is significant for obtaining the most optimal result from the evolutionary algorithm. Let G_i be the number of generations.

$$G_i = \left[X_1^i, X_2^i, X_3^i, \ldots\ldots\ldots X_{N_P}^i\right] \quad for\ CR \in [0,1], F \in [0,1] \tag{26}$$

For each solution, there are D number of parameters. The generation number is defined by i.

$$X_n^i = G_{n1}, G_{n2}, G_{n3}, \ldots\ldots\ldots G_{nD}$$

For the next two steps, each solution's objective function is determine; then, the population is nominated according to the best solution. Afterwards, the process is terminated or continued according to the stopping criteria. This step consists of mutation and crossover processes. These are the main elements of the DE algorithm. Finally, for each solution in the population, an offspring *(variant vector solution)* is generated using the following formula

$$V_i^{G+1} = X_i^G + F\left(X_{best}^G - X_i^G\right) + F(X_{r1}^G - X_{r2}^G) \tag{27}$$

where, X_{r1}^G and X_{r2}^G are two different randomly generated solution vector.X_{best}^G is the solution that has the best objective function. Next, the parameters from the parent or offspring solutions are copied to generate a trial solution. In the process, a random number is generated and compared with the crossover factor. If the generated number is bigger than that of the crossover factor, the trial solution will take the parameter from the parent; otherwise, the value from the offspring is selected. This procedure is repeated until obtaining the trial solution. For the final step, the fitness function is evaluated for the trial solutions. Then, a new solution is formed based on the trial's fitness values and original solutions. Finally, the solution with the best fitness function is taken as the new parent for the next generation round. A variety of achievement criteria are analyzed beneath the control, including the Integral of Time Absolute Error (ITAE), Integral of Squared Error (ISE), and Integral of Time multiplied Squared Error (ITSE). The ISE measures the deviation of the predicted value from the true value, the ITAE measures the deviation of the predicted value from the actual value, and the ITSE measures the deviation of the estimated value from the true value. These criteria are all used to assess control system performance. The ISE is a commonly used metric in control system analysis as it quantifies the average squared error between the predicted value and the true value. By measuring the deviation in this way, engineers are able to evaluate the accuracy of the control system's output and make necessary adjustments for optimal performance. This whole process is repeated until the stopping criteria is met or the maximum generation is reached. The following ISE formulation is considered as the objective or cost function for the problem under consideration

$$ISE = \int_0^t (\Delta f)^2\, dt \tag{28}$$

The control parameters boundaries are chosen as:

$$50 \le K_i \le 160,\ 50 \le K_p \le 160,$$
$$1 \le K_{VI} \le 7,\ and\ 1 \le D_{VI} \le 7.$$

VI. SIMULATION AND RESULTS

The simulation results were used to evaluate the effectiveness of the proposed control strategy in maintaining the MG output voltage and power factor under varying conditions. The results showed that the proposed control strategy effectively maintained the MG output voltage and power factor under different operating conditions. The MATLAB/SIMULINK platform was utilized for MG time response analysis under high penetration of RESs, loads, and parameter perturbations. The DE was used to optimize the VI controller parameters. A simulation was performed under three scenarios to

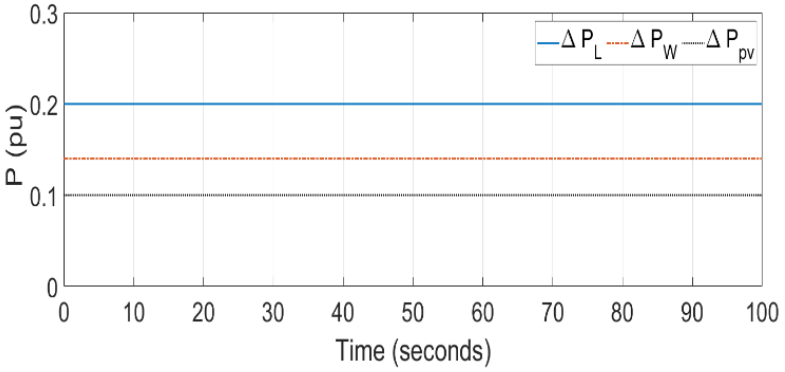

FIGURE 6. Load, wind and PV power.

TABLE 1. Optimal parameters of the VI controller.

Parameters	Optimal Values
K_p	146
K_i	145
K_{VI}	5.2
D_{VI}	5.4

demonstrate the suggested strategy's efficacy. The optimal parameters of the VI controller are shown in Table 1. The results show that DE is highly effective at finding the optimal parameters of the VI controller. This ensures a high penetration of RESs, loads, and parameter perturbations in the time domain. By optimizing parameters through the DE algorithm, the VI control technique was successfully implemented. The optimum gains of the improved derivative VI controller are designed as Virtual Inertia Emulator gain, $K_{VI} = 5.35$, Inertia and damping gain, $D_{VI} = 5.62$, Proportional control variable gain, $K_P = 148.9$, Integral control variable gain, $K_I = 146.3$ with cost function converges reaches 0.47728. The following are three simulated scenarios. Each scenario was carefully crafted to provide the most accurate results possible. The simulations were based on historical data and trends, and the results were analyzed to determine the potential outcomes of each scenario. This allowed for an in-depth analysis of the potential implications of each scenario and the most appropriate course of action. The solution vector used to solve the problem presented here consists of the gains of the improved derivative VI controller. This is KV I, DV I, KP, and KI. These gains are optimized using the DE algorithm to achieve a high penetration of RESs, loads, and parameter perturbations in the time domain. The convergence of the cost function to 0.47728 indicates the effectiveness of the optimized controller parameters.

A. SCENARIO I: CONSTANT LOADS, WIND, AND SOLAR PV POWER

This scenario uses constant load, wind, and solar PV. The constant load represents a baseline electricity demand that must be met. In addition, wind and solar PV sources can provide intermittent energy sources to supplement electricity production. This allowed for a reliable power supply that could be maintained even under changes in weather conditions. The MG response was examined under constant scenarios. The load, wind, and PV are shown in Figure 6. Figure 7 shows the response. The response was examined under the actions of the improved VI controller, the traditional VI controller, and no controller action. Traditional VI controllers were used as controller parameters, but were not considered. Figure 7 shows how frequency deviation is improved under various controls. With no control action, the transient period of the frequency deviation has a large overshoot. This is improved using a conventional VI controller but with small oscillations in the transient state in the first 10s. With our improved VI controller, both inertia and damping (D_{VI}) are added. In comparison to conventional VI controller action, the selected controller function produces a much better response with very small oscillations in the transient state. During the first 10 seconds of the enhanced VI controller, oscillations are suppressed. As a result, the improved response of the D_{VI} controller provides a much smoother transition with minimal oscillations in the first 10 seconds of operation. This improved response is sustained over a longer period of time, with excellent oscillation suppression results during the first 10s. As such, our improved VI controller with its added inertial and damping components provides significantly better performance, allowing for smooth and stable operation. In addition, the improved VI controller results in a much better response with negligible oscillations during the first 10 seconds. This makes it a clear choice over the conventional VI controller. The VI controller parameters were optimized using DE. Furthermore, the optimized controller parameters ensured that the improved VI controller had better performance than the conventional one throughout the process. Moreover, the optimized controller parameters ensured the improved VI controller had superior performance than the conventional controller in the long run.

B. SCENARIO II: UNIT STEP LOAD, WIND, AND PV POWER

A unit step signal for load, wind, and PV output was used in scenario 2 to examine the model under RES and load

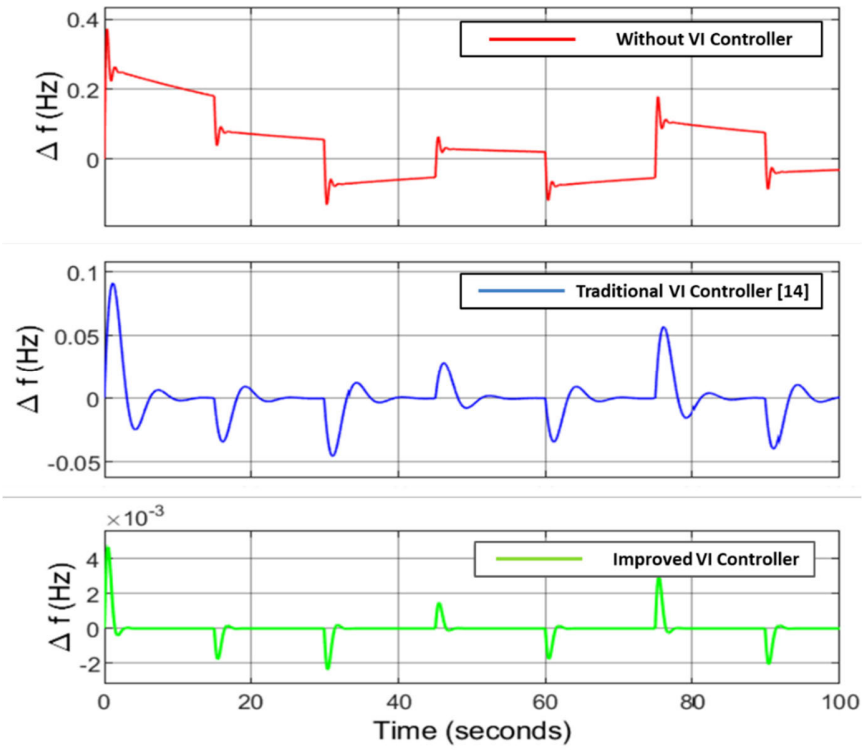

FIGURE 7. Frequency deviation for constant load, wind, and PV power.

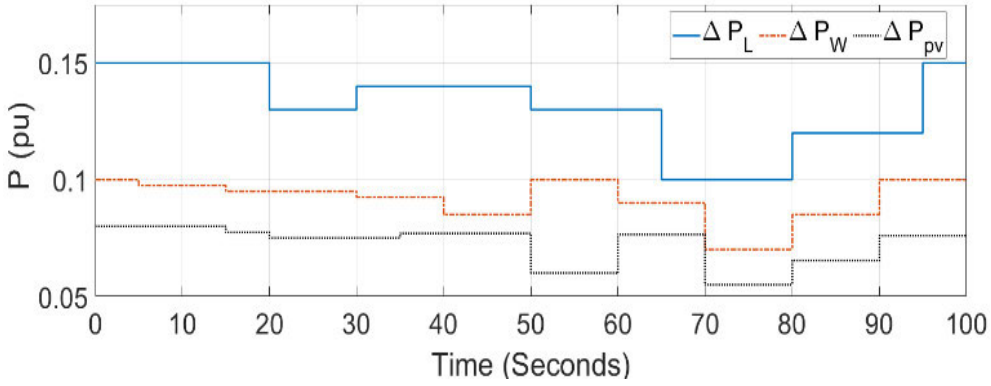

FIGURE 8. Unit step load, wind and PV power.

variability. The unit step signal enabled the model to be tested under various conditions, such as varying renewable energy sources and load changes. In this situation of high penetration of RESs and loads, the frequency deviation is higher due to lower inertia. As a result, the model's ability to maintain a stable frequency was decreased. This highlighted the need for energy storage or other technologies to offset variability. According to scenario I, the traditional VI controller and the improved VI controller (with optimal parameters) were used. Therefore, to improve system frequency stability and to ensure the dynamic performance of the system, RESs and loads must be managed appropriately. Additionally, it was found that the energy storage or other technologies must be combined with a suitable control strategy to effectively manage the variability of RESs and loads. Also, the parameters K_{VI} and D_{VI} are optimized for the improved VI controller based on DE. Figure 8 shows load, wind, and PV outputs. Based on Figure 9, the modified controller suppresses frequency deviation better than the traditional VI controller. To further improve system frequency stability and ensure the dynamic performance of the system, the parameters K_{VI} and D_{VI} can be optimized with the improved VI controller based on DE, which yields superior frequency deviation suppression as shown in Figure 9.

C. SCENARIO III: RANDOM LOAD, WIND, AND PV POWER

The model is examined here, assuming renewable energy sources will be widely adopted. In addition, more realistic

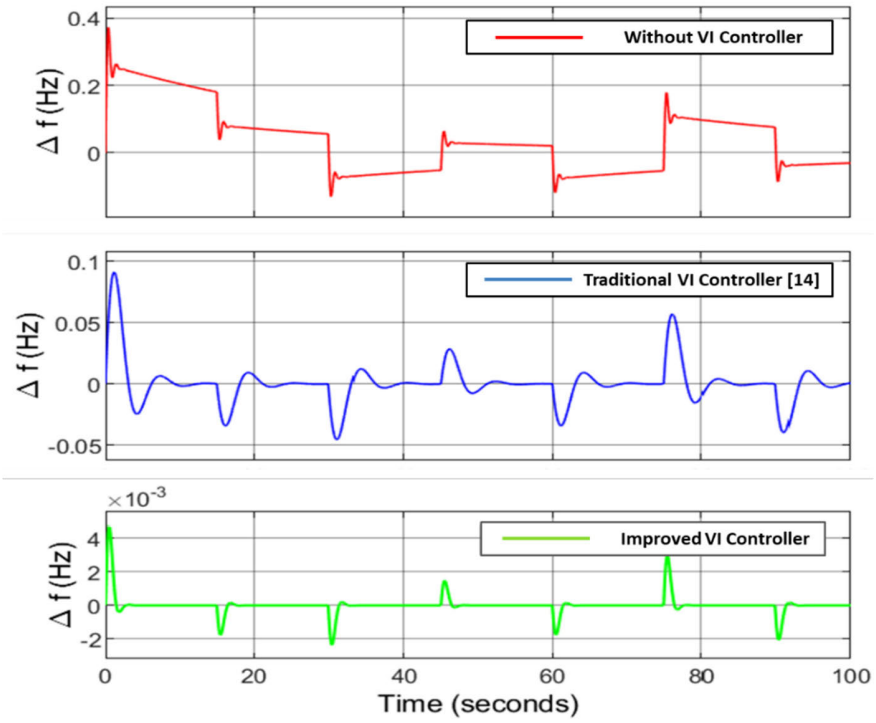

FIGURE 9. Frequency deviation for unit step load, wind and PV.

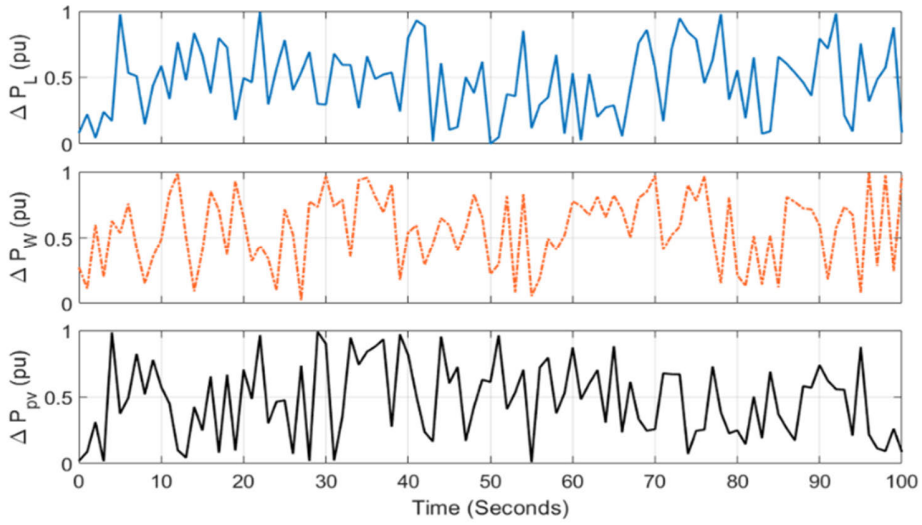

FIGURE 10. Random load, wind and PV power.

uncertainty will be associated with renewable energy sources. This is done to determine the optimal deployment of energy storage technologies and the associated system performance under these conditions. Random signals for load, wind, and PV outputs were used. During much higher penetration of RESs and loads, frequency deviation increases due to lower inertia. As such, energy storage technologies have become increasingly relevant to ensure a well-functioning electricity grid with high renewable penetration. In the first two scenarios, two different types of VI controllers (with optimal parameters) were used. Therefore, energy storage solutions become increasingly important, since they are essential to balancing the frequency variations and guaranteeing grid stability. Figure 10 shows load, wind output and PV output. As seen in Figure 11, the improved controller shows better stabilizing performance than the traditional VI controller.

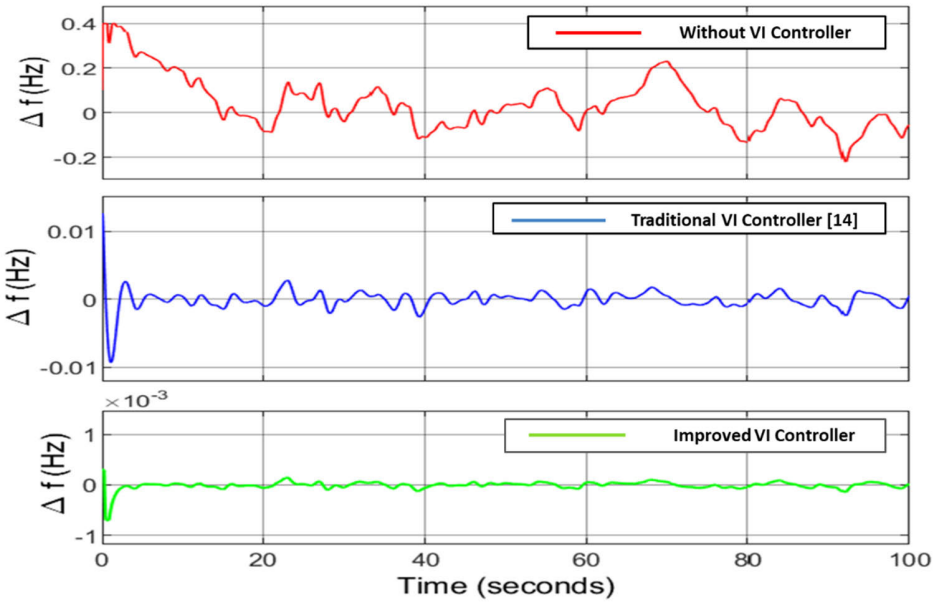

FIGURE 11. Frequency deviation for random load, wind, and PV.

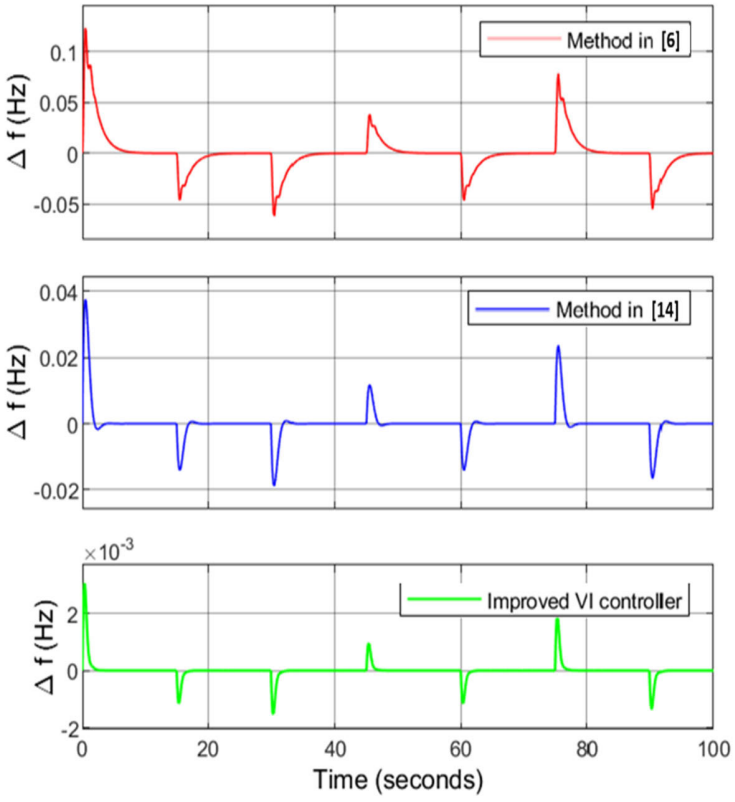

FIGURE 12. Frequency deviation comparison with pre-existing techniques.

To this end, energy storage systems play a key role in stabilizing the grid and increasing the reliability of the renewable energy sources.

This article compares the developed VI control method with some VI control techniques used in the past. It demonstrates its effectiveness in improving microgrid inertia. The results of this comparison demonstrate that the suggested method is more effective at enhancing microgrid inertia than existing methods. One of the VI control techniques used for the comparison utilizes particle

swarm optimization (PSO) [17] to optimize the controller parameters. Moreover, it is more efficient than PSO-based control methods, which makes it more suitable for small-scale microgrids. This efficiency makes the VI control method well-suited for quick and reliable implementation in small-scale microgrid systems. In [17], the damping parameter DVI was not considered. As for the comparison, the load, wind output, and PV output are the same as those of the unit step inputs in Figure 8, scenario II. The other technique used for comparison utilizes the H_∞ control theory [6] for the virtual inertia control system. Moreover, the effectiveness of the proposed VI control method has been further demonstrated by comparing it to the H_∞ control theory technique in terms of load, wind output, and PV output for the same unit step inputs. The results show that the proposed VI control system outperforms the H∞ control theory technique, confirming its effectiveness. This comparison shows that the proposed method is more suitable for microgrid applications than the PSO-based control technique. Furthermore, it offers a more robust and reliable performance in these applications. As shown in Figure 12, the proposed improved VI controller for virtual inertia produces a more accurate result. This further proves that the improved VI controller is a better choice for microgrid applications, providing better overall results. This improved VI controller demonstrates the advantages of using it in microgrid applications, as it offers superior accuracy and efficiency compared to the PSO-based control technique.

VII. CONCLUSION

In a microgrid with low inertia due to high penetration of RESs, a VI control technique was developed, which improves system stability. This control technique has been demonstrated to successfully enhance the dynamic stability of a microgrid with low inertia. This allows for higher penetration of RESs. A DE algorithm was used to optimize the parameters of the VI controller. A successful implementation of VI control was achieved through the optimization of parameters using the DE algorithm. This resulted in a more stable microgrid with a higher penetration of renewable energy sources. To demonstrate the effect of different loads, wind output, and PV output, constant, unit step, and random disturbances were applied. This showed that the controller was robust to varying conditions and ensured high reliability for the microgrid. Finally, a comparison was made between the improved VI control technique and the traditional VI control technique and other control techniques used in the past. As compared to conventional control techniques, the VI control technique showed considerable advantages, such as improved reliability and robustness to varying conditions. Due to its superior performance and reliability, VI control is clearly the optimal choice for microgrid applications. With respect to both steady and transient states, this control technique outperforms derivative VI controllers in steady and transient states. In future, the proposed control technique will be further modified for adaptive frequency contorl of renewable energy integrated microgrids.

REFERENCES

[1] X. Li, Z. Li, L. Guo, J. Zhu, Y. Wang, and C. Wang, "Enhanced dynamic stability control for low-inertia hybrid AC/DC microgrid with distributed energy storage systems," *IEEE Access*, vol. 7, pp. 91234–91242, 2019.

[2] M. Tuo and X. Li, "Optimal allocation of virtual inertia devices for enhancing frequency stability in low-inertia power systems," in *Proc. North Amer. Power Symp. (NAPS)*, College Station, TX, USA, Nov. 2021, pp. 1–6, doi: 10.1109/NAPS52732.2021.9654729.

[3] F. S. Rahman, T. Kerdphol, M. Watanabe, and Y. Mitani, "Optimization of virtual inertia considering system frequency protection scheme," *Electr. Power Syst. Res.*, vol. 170, pp. 294–302, May 2019, doi: 10.1016/j.epsr.2019.01.025.

[4] Q. Peng, Q. Jiang, Y. Yang, T. Liu, H. Wang, and F. Blaabjerg, "On the stability of power electronics-dominated systems: Challenges and potential solutions," *IEEE Trans. Ind. Appl.*, vol. 55, no. 6, pp. 7657–7670, Nov. 2019.

[5] B. Pournazarian, R. Sangrody, M. Lehtonen, G. B. Gharehpetian, and E. Pouresmaeil, "Simultaneous optimization of virtual synchronous generators parameters and virtual impedances in islanded microgrids," *IEEE Trans. Smart Grid*, vol. 13, no. 6, pp. 4202–4217, Nov. 2022, doi: 10.1109/TSG.2022.3186165.

[6] T. Kerdphol, F. S. Rahman, Y. Mitani, M. Watanabe, and S. K. Küfeoglu, "Robust virtual inertia control of an islanded microgrid considering high penetration of renewable energy," *IEEE Access*, vol. 6, pp. 625–636, 2018.

[7] J. Fang, H. Li, Y. Tang, and F. Blaabjerg, "On the inertia of future more-electronics power systems," *IEEE J. Emerg. Sel. Topics Power Electron.*, vol. 7, no. 4, pp. 2130–2146, Dec. 2019.

[8] S. Oshnoei, M. R. Aghamohammadi, S. Oshnoei, S. Sahoo, A. Fathollahi, and M. H. Khooban, "A novel virtual inertia control strategy for frequency regulation of islanded microgrid using two-layer multiple model predictive control," *Appl. Energy*, vol. 343, Aug. 2023, Art. no. 121233, doi: 10.1016/j.apenergy.2023.121233.

[9] W. Xing, H. Wang, L. Lu, X. Han, K. Sun, and M. Ouyang, "An adaptive virtual inertia control strategy for distributed battery energy storage system in microgrids," *Energy*, vol. 233, Oct. 2021, Art. no. 121155, doi: 10.1016/j.energy.2021.121155.

[10] Q.-C. Zhong and G. Weiss, "Synchronverters: Inverters that mimic synchronous generators," *IEEE Trans. Ind. Electron.*, vol. 58, no. 4, pp. 1259–1267, Apr. 2011.

[11] E. Rakhshani, D. Remon, A. Mir Cantarellas, and P. Rodriguez, "Analysis of derivative control based virtual inertia in multi-area high-voltage direct current interconnected power systems," *IET Gener., Transmiss. Distrib.*, vol. 10, no. 6, pp. 1458–1469, Apr. 2016.

[12] H. Bevrani, T. Ise, and Y. Miura, "Virtual synchronous generators: A survey and new perspectives," *Int. J. Electr. Power Energy Syst.*, vol. 54, pp. 244–254, Jan. 2014.

[13] S. D'Arco, J. A. Suul, and O. B. Fosso, "A virtual synchronous machine implementation for distributed control of power converters in smartgrids," *Electr. Power Syst. Res.*, vol. 122, pp. 180–197, May 2015.

[14] M. Joshi, G. Sharma, and E. Çelik, "Load frequency control of hydro-hydro power system using fuzzy-PSO-PID with application of UC and RFB," *Electr. Power Compon. Syst.*, vol. 51, no. 12, pp. 1156–1170, 2023, doi: 10.1080/15325008.2023.2196663.

[15] M. Joshi, G. Sharma, P. N. Bokoro, and N. Krishnan, "A fuzzy-PSO-PID with UPFC-RFB solution for an LFC of an interlinked hydro power system," *Energies*, vol. 15, no. 13, p. 4847, Jul. 2022, doi: 10.3390/en15134847.

[16] K. S. Ratnam, K. Palanisamy, and G. Yang, "Future low-inertia power systems: Requirements, issues, and solutions—A review," *Renew. Sustain. Energy Rev.*, vol. 124, May 2020, Art. no. 109773, doi: 10.1016/j.rser.2020.109773.

[17] G. Magdy, G. Shabib, A. A. Elbaset, and Y. Mitani, "A novel coordination scheme of virtual inertia control and digital protection for microgrid dynamic security considering high renewable energy penetration," *IET Renew. Power Gener.*, vol. 13, no. 3, pp. 462–474, Feb. 2019.

[18] T. Kerdphol, M. Watanabe, K. Hongesombut, and Y. Mitani, "Self-adaptive virtual inertia control-based fuzzy logic to improve frequency stability of microgrid with high renewable penetration," *IEEE Access*, vol. 7, pp. 76071–76083, 2019.

[19] T. Kerdphol, F. S. Rahman, M. Watanabe, Y. Mitani, D. Turschner, and H.-P. Beck, "Enhanced virtual inertia control based on derivative technique to emulate simultaneous inertia and damping properties for microgrid frequency regulation," *IEEE Access*, vol. 7, pp. 14422–14433, 2019.

[20] T. Chen, J. Guo, B. Chaudhuri, and S. Y. Hui, "Virtual inertia from smart loads," *IEEE Trans. Smart Grid*, vol. 11, no. 5, pp. 4311–4320, Sep. 2020.

[21] K. Shi, W. Song, H. Ge, P. Xu, Y. Yang, and F. Blaabjerg, "Transient analysis of microgrids with parallel synchronous generators and virtual synchronous generators," *IEEE Trans. Energy Convers.*, vol. 35, no. 1, pp. 95–105, Mar. 2020.

[22] W. M. Hamanah, M. A. Abido, and L. M. Alhems, "Optimum sizing of hybrid PV, wind, battery and diesel system using lightning search algorithm," *Arabian J. Sci. Eng.*, vol. 45, no. 3, pp. 1871–1883, Mar. 2020, doi: 10.1007/s13369-019-04292-w.

[23] M. L. Hennache, W. M. Hamanah, and A. Mohammad, "PV inverter control design for mitigating fault-induced delayed voltage recovery (FIDVR)," in *Proc. IEEE Int. Conf. Energy Technol. Future Grids (ETFG)*, Wollongong, NSW, Australia, Dec. 2023, pp. 1–6, doi: 10.1109/ETFG55873.2023.10407851.

[24] H. Xu, C. Yu, C. Liu, Q. Wang, and X. Zhang, "An improved virtual inertia algorithm of virtual synchronous generator," *J. Mod. Power Syst. Clean Energy*, vol. 8, no. 2, pp. 377–386, Mar. 2020.

[25] E. Rakhshani, D. Remon, A. M. Cantarellas, J. M. Garcia, and P. Rodriguez, "Virtual synchronous power strategy for multiple HVDC interconnections of multi-area AGC power systems," *IEEE Trans. Power Syst.*, vol. 32, no. 3, pp. 1665–1677, May 2017.

[26] R. Mandal and K. Chatterjee, "Frequency control and sensitivity analysis of an isolated microgrid incorporating fuel cell and diverse distributed energy sources," *Int. J. Hydrogen Energy*, vol. 45, no. 23, pp. 13009–13024, Apr. 2020, doi: 10.1016/j.ijhydene.2020.02.211.

[27] R. Mandal and K. Chatterjee, "Virtual inertia emulation and RoCoF control of a microgrid with high renewable power penetration," *Electr. Power Syst. Res.*, vol. 194, May 2021, Art. no. 107093, doi: 10.1016/j.epsr.2021.107093.

[28] Q. Peng, Y. Yang, T. Liu, and F. Blaabjerg, "Coordination of virtual inertia control and frequency damping in PV systems for optimal frequency support," *CPSS Trans. Power Electron. Appl.*, vol. 5, no. 4, pp. 305–316, Dec. 2020.

[29] M. Hajiakbari Fini and M. E. Hamedani Golshan, "Determining optimal virtual inertia and frequency control parameters to preserve the frequency stability in islanded microgrids with high penetration of renewables," *Electr. Power Syst. Res.*, vol. 154, pp. 13–22, Jan. 2018, doi: 10.1016/j.epsr.2017.08.007.

[30] K. Liu, Y. Qu, H.-M. Kim, and H. Song, "Avoiding frequency second dip in power unreserved control during wind power rotational speed recovery," *IEEE Trans. Power Syst.*, vol. 33, no. 3, pp. 3097–3106, May 2018.

[31] E. Alzahrani, M. Shafiullah, W. M. Hamanah, and M. A. Abido, "Equilibrium optimizer for community microgrid energy scheduling," in *Proc. IEEE Ind. Electron. Appl. Conf. (IEACon)*, Penang, Malaysia, Nov. 2023, pp. 110–115, doi: 10.1109/IEACon57683.2023.10370060.

[32] W. M. Hamanah, A. Baraean, A. Hussein, and M. A. Abido, "Stabilizing multimachine power systems with fuzzy logic using artificial bee colonies," *Renew. Energy Power Qual. J.*, vol. 21, no. 1, pp. 166–171, Jul. 2023, doi: 10.24084/repqj21.258.

[33] A. Baraean, W. M. Hamanah, A. Bawazir, M. M. Quama, S. E. Ferik, S. Baraean, and M. A. Abido, "Optimal nonlinear backstepping controller design of a quadrotor-slung load system using particle swarm optimization," *Alexandria Eng. J.*, vol. 68, pp. 551–560, Apr. 2023, doi: 10.1016/j.aej.2023.01.050.

[34] X. Zhang, Z. Zhu, Y. Fu, and L. Li, "Optimized virtual inertia of wind turbine for rotor angle stability in interconnected power systems," *Electr. Power Syst. Res.*, vol. 180, Mar. 2020, Art. no. 106157, doi: 10.1016/j.epsr.2019.106157.

[35] P. Rodríguez, C. Citro, J. I. Candela, J. Rocabert, and A. Luna, "Flexible grid connection and islanding of SPC-based PV power converters," *IEEE Trans. Ind. Appl.*, vol. 54, no. 3, pp. 2690–2702, May 2018.

[36] C. Verdugo, A. Tarraso, J. I. Candela, J. Rocabert, and P. Rodriguez, "Centralized synchronous controller based on load angle regulation for photovoltaic power plants," *IEEE J. Emerg. Sel. Topics Power Electron.*, vol. 9, no. 1, pp. 485–496, Feb. 2021.

[37] T. Kerdphol, F. S. Rahman, M. Watanabe, and Y. Mitani, "Robust virtual inertia control of a low inertia microgrid considering frequency measurement effects," *IEEE Access*, vol. 7, pp. 57550–57560, 2019, doi: 10.1109/ACCESS.2019.2913042.

[38] A. Rai and R. Dahiya, "A virtual inertia control schemes for DC microgrids in grid connected mode," in *Proc. Int. Conf. Power Energy, Environ. Intell. Control (PEEIC)*, Greater Noida, India, Apr. 2018, pp. 96–101, doi: 10.1109/PEEIC.2018.8665466.

[39] F. Perez, G. Damm, C. M. Verrelli, and P. F. Ribeiro, "Adaptive virtual inertia control for stable microgrid operation including ancillary services support," *IEEE Trans. Control Syst. Technol.*, pp. 1–13, Jan. 2023, doi: 10.1109/TCST.2023.3234282.

[40] N. Meenakshi and D. Kavitha, "Optimized self-healing of networked microgrids using differential evolution algorithm," in *Proc. Nat. Power Eng. Conf. (NPEC)*, Madurai, India, Mar. 2018, pp. 1–7, doi: 10.1109/NPEC.2018.8476779.

[41] X. Qian, Y. Yang, C. Li, and S.-C. Tan, "Operating cost reduction of DC microgrids under real-time pricing using adaptive differential evolution algorithm," *IEEE Access*, vol. 8, pp. 169247–169258, 2020, doi: 10.1109/ACCESS.2020.3024112.

[42] A.-W.-A. Saif, A. Aliyu, M. A. Dhaifallah, and M. Elshafei, "Decentralized backstepping control of a quadrotor with tilted-rotor under wind gusts," *Int. J. Control, Autom. Syst.*, vol. 16, no. 5, pp. 2458–2472, Oct. 2018.

WALEED M. HAMANAH received the B.Sc. degree in electrical engineering in Sana'a, Yemen, in June 2008, and the M.Sc. and Ph.D. degrees in electrical engineering from the King Fahd University of Petroleum and Minerals (KFUPM), Dhahran, Saudi Arabia, in 2016 and 2021, respectively. He was an Instructor with Taiz University, Yemen, from September 2008 to December 2011. He was a Postdoctoral Researcher with the Interdisciplinary Research Center for Renewable Energy and Power Systems (IRC-REPS), Research and Innovation, KFUPM. He is currently with the ARC-MST Research Institute, KFUPM, as a Research Engineer III (Assistance Professor). His research interests include renewable energy, power electronics, high voltage, energy storage microgrids, machines, intelligent control, and saving energy.

MD. SHAFIULLAH (Senior Member, IEEE) received the B.Sc. and M.Sc. degrees in electrical and electronic engineering (EEE) from Bangladesh University of Engineering and Technology (BUET), Bangladesh, in 2009 and 2013, respectively, and the Ph.D. degree in electrical power and energy systems from the King Fahd University of Petroleum and Minerals (KFUPM), Saudi Arabia, in 2018. He was a Faculty Member with the Department of Electrical and Electronic Engineering, International Islamic University Chittagong (IIUC), Bangladesh, from 2009 to 2013. He is currently an Assistant Professor with the Control and Instrumentation Department and a Research Affiliate with the Interdisciplinary Research Center for Renewable Energy and Power Systems (IRC-REPS), KFUPM. His research interests include grid fault diagnosis, grid integration of renewable energy resources, power quality analysis, power system control and stability, evolutionary algorithms, and machine learning techniques.

LUAI M. ALHEMS received the B.Sc. (Hons.) and M.Sc. degrees in ME from the King Fahd University of Petroleum and Minerals, Dhahran, Saudi Arabia, in 1994 and 1997, respectively, and the Ph.D. degree from Texas A&M University, College Station, TX, USA, in 2002. In addition to his role as the Director of the Applied Research Center for Metrology, Standards and Testing, he is also the Director of the Applied Research Center for Environment and Marine Studies. He has published 25 patents and more than 200 research articles. He participated in more than 50 funded projects and supervised more than 30 M.S. and Ph.D. students. His research interests include mechanical engineering, thermo fluid, fouling, wind/solar energy, heat transfer and thermodynamics, multiphase, and energy conservation. He was a recipient of the KFUPM Excellence in Research Project Team Award in 2014 and the Almarai Prize for Scientific Innovation in 2015. He received Dubai Quality Group Energy Engineer Award in 2007 from HH Shaikh Mohamed bin Rashid Al-Maktoum (Vice President of United Arab Emirates and the Prime Minister and the Ruler of Dubai) in a ceremony held in Dubai.

MD. SHAFIUL ALAM received the B.Sc. degree in electrical and electronic engineering (EEE) from Dhaka University of Engineering and Technology, Gazipur, Bangladesh, the M.Sc. degree in EEE from Bangladesh University of Engineering and Technology, Dhaka, Bangladesh, and the Ph.D. degree in electrical engineering from the King Fahd University of Petroleum and Minerals (KFUPM), Saudi Arabia. In August 2008, he started his career as a Faculty Member with the Department of EEE, International Islamic University Chittagong (IIUC), Bangladesh, where his highest rank was an Associate Professor. From March 2020 to March 2022, he was a Postdoctoral Fellow with the KACARE Energy Research and Innovation Center (ERIC), KFUPM. He is currently a Research Engineer III with the Applied Research Center for Environment and Marine Studies (ARCEMS), Research Institute, KFUPM. He involved in several funded projects during the Ph.D. research. His research interests include energy and environment, greenhouse gas emission management, data analysis, renewable energy sources integration into the utility grids, ac/dc microgrids, high-voltage dc transmission, voltage source converter control, fault current limiter, optimization algorithms, fuzzy logic, neural networks, and machine learning. He is a member of the Institution of Engineers Bangladesh. He was a recipient of the best paper awards at many IEEE international conferences.

MOHAMMAD A. ABIDO (Senior Member, IEEE) received the B.Sc. (Hons.) and M.Sc. degrees in EE from Menoufia University, Shebeen El-Kom, Egypt, in 1985 and 1989, respectively, and the Ph.D. degree from the King Fahd University of Petroleum and Minerals (KFUPM), Dhahran, Saudi Arabia, in 1997. He is currently a Distinguished University Professor with KFUPM and a Senior Researcher with KACARE (ERIC), Dhahran. He has published two books and more than 350 research articles. He participated in more than 50 funded projects and supervised more than 50 M.S. and Ph.D. students. His research interests include power system stability, planning, and optimization techniques applied to power systems. He was a recipient of the KFUPM Excellence in Research Award, in 2002, 2007, and 2012; the KFUPM Best Project Award, in 2007 and 2010; the First Prize Paper Award from the Industrial Automation and Control Committee of the IEEE Industry Applications Society, in 2003; the Abdel-Hamid Shoman Prize for Young Arab Researchers in Engineering Sciences, in 2005; the Best Applied Research Award of 15th GCC-CIGRE Conference, Abu Dhabi, United Arab Emirates, in 2006; and the Best Poster Award from the International Conference on Renewable Energies and Power Quality (ICREPQ'13), Bilbao, Spain, in 2013. He has been awarded the Almarai Prize for Scientific Innovation, Distinguished Scientist, Saudi Arabia, in 2018, and the Khalifa Award for Education, Higher Education, Distinguished University Professor in Scientific Research, Abu Dhabi, in 2018.